

Analytical Methods

Accepted Manuscript



This is an *Accepted Manuscript*, which has been through the Royal Society of Chemistry peer review process and has been accepted for publication.

Accepted Manuscripts are published online shortly after acceptance, before technical editing, formatting and proof reading. Using this free service, authors can make their results available to the community, in citable form, before we publish the edited article. We will replace this *Accepted Manuscript* with the edited and formatted *Advance Article* as soon as it is available.

You can find more information about *Accepted Manuscripts* in the [Information for Authors](#).

Please note that technical editing may introduce minor changes to the text and/or graphics, which may alter content. The journal's standard [Terms & Conditions](#) and the [Ethical guidelines](#) still apply. In no event shall the Royal Society of Chemistry be held responsible for any errors or omissions in this *Accepted Manuscript* or any consequences arising from the use of any information it contains.

1
2
3 **Styrofoam modified paper as a low-cost platform for qualitative and semi-quantitative**
4 **determination of Ni²⁺ ions in wastewater**
5

6 Muhammad Imtiaz Rashid,^{a, c§} Liyakat Hamid Mujawar,^{*a§} Iqbal M. I. Ismail,^{a, b} and Mohammad Soror El-
7 Shahawi^{a, b}
8

9 ^a Center of Excellence in Environmental Studies, King Abdulaziz University, P.O Box 80216,
10 Jeddah 21589, Saudi Arabia
11

12 ^b Department of Chemistry, Faculty of Science, King Abdulaziz University, P. O. Box 80203,
13 Jeddah 21589, Saudi Arabia
14

15 ^c Department of Environmental Sciences, COMSATS Institute of Information Technology,
16 61100, Vehari, Pakistan
17
18

19
20
21 §Equal contribution
22
23
24
25
26
27
28
29
30
31
32
33
34
35
36
37
38
39
40
41
42
43
44
45

46 ***Corresponding author:**
47

48 **Liyakat Hamid Mujawar, PhD**
49

50 King Abdulaziz University,
51 Center of Excellence in Environmental Studies,
52 P.O Box 80216,
53 Jeddah 21589, Saudi Arabia
54 E-mail: lmujawar@kau.edu.sa / liyakat.mujawar@gmail.com
55 Phone: +966(12)6402000
56 Fax: +966(12)6951674
57
58
59
60

Abstract:

In the present article we have demonstrated a swift and low-cost method to design hydrophobic paper and its potential application for the determination of Ni²⁺ ions in wastewater. Styrofoam was used as a precursor to fabricate pristine filter paper into a low wetting substrate. The water contact angle (θ) of the modified paper was $\sim 111^\circ$ whereas atomic force microscopy analysis ensured a uniform coating of the polymer onto cellulose fibers. Metal specific reagent 1-(2-mercaptophenyl)iminomethyl naphthalen-2-ol (MPMN) was manually arrayed and one-step assay for the determination of Ni²⁺ was demonstrated on aforementioned substrates. End-result was observed in form of a distinct color change which was easily readable via naked eyes. We also quantitated the concentration of Ni²⁺ ions through flatbed scanning and scoring their pixel gray volume using image analysis software. On styrofoam modified paper, the limit of detection was improved to $10^{-2} \mu\text{g mL}^{-1}$, which was 3-order of magnitude lower than that observed on pristine filter paper. The MPMN reagent was highly selective towards Ni²⁺ in presence of high concentration of commonly diverse heavy metals (Ag⁺, Al³⁺, As³⁺, Ba²⁺, Cd²⁺, Cr³⁺, Fe³⁺, Pb²⁺ and Mn²⁺) and some other ions (Na⁺, Ca²⁺, K⁺ and Cl⁻) in water. Our developed method successfully demonstrated the semi-quantitative determination of Ni²⁺ ions in tap and municipal wastewater samples. Due to good specificity as well as accuracy towards Ni²⁺ ion, our low-cost sensor will be useful in point-of-use applications.

Keywords: Cellulose surface; hydrophobic; nickel; paper-based sensor; rapid assay; styrofoam.

1. Introduction:

Multivalent transitional metal ions such as Ni^{2+} , Hg^{2+} , Cd^{2+} , Co^{2+} , Fe^{3+} , Cu^{2+} occur in both natural and contaminated environments (soil, air and water). These heavy metal ions could not be easily detoxified by microbial degradation, therefore their persistence rate in the environment is higher than other elements. Most of these metal ions act as carcinogens which cause several diseases in humans^{1, 2} that in turn lead to the failure of heart, kidneys, lungs and immune system.³ Thus efficient monitoring of such toxic species is of great importance in order to prevent the living organisms from chemical pollution. Efficient screening of heavy metal ions by atomic absorption spectrophotometry is a commonly used method in addition to other available techniques such as ICP-MS,⁴ SPR,^{5, 6} QCM⁷ and atomic absorption spectroscopy.⁸ Even though most of these instruments are known to be sensitive and accurate; however their complexity in sample preparation requires significant time and high degree of expertise. Due to aforementioned factors, the application of such expensive instruments is limited to laboratory usage only.

Recently, paper-based platforms have emerged as a promising tool in sensor applications. The advantage lies in their simple design, easy operation with minimum usage (i.e., low volume) of analytes or reagent and has been successfully employed for point-of-use testing of various analytes.⁹⁻¹¹ Colorimetric read-out and low cost of these devices make them successful for field application. However, one of the major drawbacks is the complexity of the method involved in the fabrication^{12, 13} such as designing microfluidic channels onto the substrate surface in order to improve the assay sensitivity.^{11, 12, 14} Even then, most of these paper-based sensors could not detect heavy metal ions up to maximum allowable limit set by World Health Organization (WHO).¹⁵

To overcome this issue, researchers have extensively demonstrated the application of nanomaterial on microfluidic paper-based devices to enhance the limit of detection for heavy metal ions.¹⁶⁻¹⁸ Although, the amount of nanomaterial (i.e., gold) used in these devices was low nevertheless this also includes an additional step and an elevated cost in sensor preparation. Hence there is pressing need to develop powerful low-cost analytical disposable tool which has a strong sensitivity to detect heavy metals ions.

Cellulose based materials such as filter papers are known to be hydrophilic in nature with high capillary forces. However by using hexamethyldisilazane,¹⁹ wax²⁰ and polystyrene,²¹ a

highly hydrophilic material can be transformed to a hydrophobic substrate. Such low-wetting substrates have wide applications in packaging, oil separation as well as for producing hydrophobic barriers in a microfluidic chip.²²⁻²⁴ Our main interest is in the latter application as we intend to design a low-cost hydrophobic platform for sensitive determination of heavy metal ion. Therefore the main objectives of our study are: I) Fabrication of low-cost filter paper to a hydrophobic platform by using futile material such as styrofoam. II) Testing the applicability of modified paper into one step detection of Ni²⁺ ions using selective MPMN reagent (Figure 1-A) III) To determine the color intensity of assay spots by digitalizing them through flatbed scanner and scoring the pixel gray volumes (PGV) and finally, IV) to check the feasibility of our developed method in real sample analysis.

2. Materials and methods:

2.1. Reagents and materials

Whatman filter paper (Grade 5) was obtained from GE Whatman (Buckinghamshire, UK). Ni(NO₃)₂·6H₂O was purchased from BDH (Doha, Qatar) and 1-(2-mercaptophenyl)iminomethyl)naphthalen-2-ol reagent was delivered by Aldrich (St.Louis, MO, USA) (Figure 1-A). 0.25% (w/v) MPMN was prepared using minimum amount of DMF²⁵ and ethanol which was further used as a reagent for the detection of Ni²⁺. Blocks of trivial styrofoam were obtained from the packing of various instrument available at the storeroom of the Centre of Excellence in Environmental studies. They were used without any further treatment and pre-modification.

Figure 1

2.2. Apparatus:

The electronic absorption spectra of the free reagent MPMN and its complex with Ni²⁺ were recorded by a double beam spectrophotometer (190-1100 nm) with 3 cm (path width) quartz cell (Shimadzu UV1800-240V, Kyoto, Japan). Fourier transform infra-red (Shimadzu IRAffinity-1, Kyoto, Japan) was used for recording the IR spectra of the reagent and its complex with Ni²⁺. The surface topography and roughness of the pristine and modified filter paper substrates were characterized by non-contact mode atomic force microscopy (AFM). This equipment scanned 256 lines at a frequency of 0.4Hz) 20 μm × 20 μm area of pristine filter before and after modification using Park Systems NX10 AFM (Suwon, South Korea). A Milli-Q

Plus system (Millipore, Bedford, MA, USA) was used for providing deionized water. Static contact angle (θ) of a sessile water droplet on modified hydrophobic surface was measured by a Krüss contact angle measuring system (DSA30S, Hamburg, Germany).

2.3. Modification of filter paper to hydrophobic substrate

Whatman filter paper was cut into strips (12 cm \times 1.5 cm) and placed in a clean petri dish. Styrofoam was dissolved in chloroform and 1.0% (w/v) solution was prepared in the same solvent. Filter paper strips were soaked into the styrofoam solution to ensure complete coating of polymer on the cellulose fibers. The modified filter paper was air-dried for 30 min.

2.4. Recommended procedures

2.4.1. Contact angle analysis:

1 μ L Milli-Q water droplet was injected at three different places on each surface and Tangent-1 (T-1) method was used to measure θ through drop analysis software (DSA-4). The mean contact angle was reported along with the (\pm) standard deviation.

2.4.2. One step assay:

MPMN reagent was manually arrayed on pristine and styrofoam modified paper using Capp pipette (Odense S, Denmark) where the ejected volume was \sim 400 nL. The patterned substrates were allowed to air dry for 15 min to ensure complete drying of reagent spots. Simultaneously, $10^3 \mu\text{g mL}^{-1}$ standard stock solution of Ni^{2+} was prepared in MQ water which was further serially (10^2 , 10^1 , 1, 10^{-1} , $10^{-2} \mu\text{g mL}^{-1}$) diluted. On pristine paper, 3 μ L of aqueous Ni^{2+} solution was supplied, whereas in case of modified paper the supplied volume was 7 μ L. In order to accelerate the drying process paper strips was incubated at 45 $^\circ\text{C}$ for 5 min.

2.4.3. Flat-bed scanning and image analysis:

The color intensity of the reagent and assay spots was digitalized by scanning the paper strips using a flatbed scanner (Fujitsu, fi-6230Z, Japan). The scanner was set at a 24-bit color scale with resolution of 1200 dpi. Spot intensity of the scanned images was calculated using image analysis software (ImageJ). Pixel gray volume (PGV) of each spot was measured by placing a circular region of interest at the circumference of the colored area. Average PGV was calculated from three sets of individual experiments at respective concentrations.

2.4.4. Influence of dissolved carbon in water on the proposed method:

To study the influence of dissolved carbon on the developed method, the following procedures were carried out as follows:

- a. An accurate volume of water sample that was previously spiked with known concentration ($10 \mu\text{g mL}^{-1}$) of analyte was analyzed for the determination of Ni^{2+} following the recommended procedures. The PGV obtained for the assay spot was measured as I_1 .
- b. Another experiment for identical spiked water sample was digested with HCl (10% v/v) in the presence of H_2O_2 (30%v/v) and boiling for approximately 1h. After complete digestion and adjustment of pH and sample volume, the sample was then analyzed by our developed method for the determination of Ni^{2+} . Finally we have recorded the PGV of Ni^{2+} in the digested sample as I_2 .

2.4.5. Analytical applications:

The feasibility of styrofoam modified filter paper on the detection and semi-quantitative determination of Ni^{2+} ions in tap- and municipal waste water samples was carried out. To judge the performance in real sample analysis, domestic tap water was spiked with $1 \mu\text{g mL}^{-1}$ of Ni^{2+} and the concentration of the heavy metal ions was determined through proposed one-step assay. We also analyzed the concentration of metal ions in wastewater. Samples were collected from four different locations in the Kingdom of Saudi Arabia which were used without any pre-treatment. The assay procedure was followed in accordance as explained in section 2.4.2.

3. Results and discussion

3.1. Atomic force microscopy (AFM) analysis

Surface modification of pristine filter paper with solubalized styrofoam transforms the hydrophilic substrate to a hydrophobic platform. This was also confirmed by goniometer analysis which showed an increase in contact angle (θ) for a high absorbing pristine paper to $110.9 \pm 0.5^\circ$. Although no significant differences in the physical appearance of modified and pristine paper was observed, but still we characterized the influence of styrofoam modification on the topography of pristine and modified paper by AFM (non-contact mode). Microscopy analysis revealed that in pristine filter paper the cellulose fibers were more prominent and sharp as shown in Figure 2-A, B (Pristine). Upon modification, similar fibrous structures showed a subdued

morphology as a uniform layer of polymer was masked on to the cellulose matrix (Figure 2-A, B; Styrofoam modified).

A significant difference was also observed on the surface roughness (i.e., R_a and R_q) of the pristine and styrofoam modified papers. As compared to the former, the R_a and R_q of latter were increased by 52% and 56%, respectively (Figure 2-C). By manual inspection, the modified surface was found to be more firm as compared to unmodified one. This was reflected in AFM analysis where we found an increase in the stiffness (~ 1.6 to ~ 1.7 N m⁻¹) as well as adhesion values ($\sim 54 \times 10^{-18}$ to $\sim 85 \times 10^{-18}$ J) of hydrophobic paper (Figure 2-D, E).

Figure 2

3.2. One step assay for the detection of Ni^{2+} ion:

The application of styrofoam modified paper as a platform for sensitive and rapid detection of Ni^{2+} was also demonstrated. Upon interaction of aqueous Ni^{2+} ion with the arrayed MPMN spots, a yellowish brown colored complex was developed. Complex formation was also confirmed from the observed bathochromic shift of the absorptions peaks at 300, 315 and 328 nm ($n \rightarrow \pi^*$) in the electronic spectrum of the reagent to 380(w) and 454(s) nm for the Ni^{2+} complex (Supplementary information, SI-1). The peaks recorded at 380 (w) and 454(s) nm in the spectrum of Ni^{2+} complex are safely assigned to $^1A_{1g} \rightarrow ^1B_{1g}$ and $^1A_{1g} \rightarrow ^1A_{2g}$ d-d transitions in square planar geometry.²⁶ On the other hand, the reagent MPMN (Figure 1-A) has three binding sites (-OH, -C=N- and SH) in complex formation with metal ions. The assignment of the FTIR bands of the free reagent and its Ni-MPMN complex is determined by careful comparison with the FTIR spectra of similar reagents and their Ni^{2+} complexes.²⁷ A comparison of the IR spectra of the reagent and its Ni-complex has revealed that, the reagent participated to Ni^{2+} as a monobasic acid in a bidentate fashion through mercapto sulfur $\nu(-SH)$ after deprotonation as indicated from the disappearance of νSH (2623 cm⁻¹) of the free reagent in complex formation.²⁸ Coordination of $\nu(-C=N)$ nitrogen of the reagent was also noticed from the observed shift of $\nu C=N$ at 1613 cm⁻¹ of the free reagent to lower frequency (16015 cm⁻¹) in complex formation. The appearance of vibrations at 460 ν M-O and 355 cm⁻¹ ν M-S in the complex which are absent in the spectrum of the free reagent and the appearance of the IR band at $3450-3470$ cm⁻¹ in the free MPMN and Ni-MPMN complex which is safely assigned to phenolic ν O-H group added further support for participation of SH and (-C=N) nitrogen. Thus, it can be concluded that the MPMN coordinated to Ni^{2+} via mercapto (-SH) sulfur and azomethine (-C=N) nitrogen forming six-

1
2
3
4
5
6
7
8
9
10
11
12
13
14
15
16
17
18
19
20
21
22
23
24
25
26
27
28
29
30
31
32
33
34
35
36
37
38
39
40
41
42
43
44
45
46
47
48
49
50
51
52
53
54
55
56
57
58
59
60

membered ring chelate in 1:2 (Ni:MPMN) molar ratio as shown in Figure 1-B. The electronic and FTIR spectra of the reagent and its Ni(MPMN)₂ chelate were individually performed and included in SI-1 and SI-2, respectively.

As shown in Figure 3-A (inset), the limit of detection (LOD) on the pristine filter paper was only 10¹ µg mL⁻¹ as no color formation was visible on the reagent spots below this concentration. The color intensity of the spots above 10¹ µg mL⁻¹ increased proportionally with the metal ion concentration. However, the sensitivity was greatly improved when similar assay was executed on styrofoam modified filter paper. When compared with the blank spot, a distinct brown color formation was easily visible for 10⁻² µg mL⁻¹ concentration of Ni²⁺. With increasing concentration of heavy metal ion, the color of the Ni-reagent complex increased proportionally from 10⁻² - 10³ µg mL⁻¹ (Figure 3-B, inset). As compared to pristine paper, the limit of detection on modified paper was lower by 3-order of magnitude.

Figure 3

The observed difference in assay sensitivity is mainly attributed due to the liquid confinement of the analyte droplet onto the substrate surface. The spreading behavior for the reagent and analyte solution on both paper substrates is listed in Table 1. On pristine filter paper a 100% coverage of Ni²⁺ solution (1000 and 100 µg mL⁻¹) on the reagent spot was observed. For similar analyte concentrations, the total coverage of reagent spot by aqueous Ni²⁺ droplet on modified paper was ~60% (1000 µg mL⁻¹) and 57% (100 µg mL⁻¹), respectively. This shows that low wettability of styrofoam modified paper limits the spreading of analyte droplet to a confined area. Even though on modified paper the supplied analyte volume was three times higher, but the total coverage was almost half as compared to that observed on pristine paper.

Table 1

Due to low wettability of the modified substrate, the aqueous metal ion droplet is restricted to diffuse freely in XYZ direction. This liquid confinement allows more number of analyte molecules to react on the reagent spot thus resulting in a cumulative signal density. A contrasting phenomenon occurs on the pristine filter paper where the hydrophilic nature of the substrate allows excessive spreading of aqueous (analyte) droplet not only in XY but also in Z direction. This may have negligible effect at high analyte concentration as a strong colored

1
2
3 complex formation is observed at $100 \mu\text{g mL}^{-1} \text{Ni}^{2+}$ (Figure 3-A). However, at low
4 concentrations this may be critical as the formation of colored complex is weak and unable to
5 read via naked eyes or image analysis software.
6
7

8
9 These results are in agreement with Ekin's 'Ambient analyte theory'^{29, 30} that states the
10 signal in a microspot increases with higher density of capture molecules as well as spot size
11 whereas the signal density is inversely proportional to the density of capture molecules and spot
12 size. These observations are in accordance with findings of Mujawar *et al.*^{25, 31} who found higher
13 signal density and signal-to-noise ratio on hydrophobic glass ($\theta > 90^\circ$) as compared to pristine
14 substrate in diagnostic immunoassays. Recently, Feng *et al.*¹³ also demonstrated an enhancement
15 in the sensitivity for a paper-based assay by supplying higher volume of analyte solution to the
16 reagent. Additionally, the detection was based on UV-LED array and LOD of their system for
17 Ni^{2+} ion was $1 \mu\text{g mL}^{-1}$. On the other hand, our low-cost modified paper could easily detect 2-
18 order of magnitude lower concentration for Ni^{2+} without any need of high-end readers. In this
19 manner we can implement our proposed modified platform in sensitive detection of various
20 analytes molecules which require low volumes of expensive reagents for their analysis.
21
22
23
24
25
26
27
28
29
30

31 3.3. Quantitative analysis of assay spots:

32
33 We also appraised the reproducibility of our developed method by performing three sets
34 of experiments on pristine and modified filter paper. The color intensity of the assay spots was
35 scored in terms of pixel gray volume (PGV) using ImageJ software. Quantitative data analysis
36 presented in Figure 3 show that the PGV values for Ni^{2+} assay on pristine paper was low as
37 compared to modified one. As seen in Figure 3-A (inset), the colored complex was only
38 observed for the concentrations above $10^1 \mu\text{g mL}^{-1}$ hence no PGV values were calculated for the
39 spots below aforementioned concentration (Figure 3-A, data plot). ImageJ is well-equipped to
40 quantitate the available pixels in any given region of interest but no PGV value denotes a
41 complete absence of colored complex formation on the reagent spot. Hence this would also
42 signify the incompetency of pristine paper in sensitive detection of Ni^{2+} ions. However, on
43 hydrophobic paper the average PGV was found to gradually increase from $10^{-2} \mu\text{g mL}^{-1}$ up to 10^3
44 $\mu\text{g mL}^{-1}$ (Figure 3-B). As the trend of the PGV values with respect to Ni^{2+} concentrations was in
45 form of an elongated S-shaped, therefore we obtained two slopes, $S1_{(0.01-1)}$ ($y = 3.1633\ln(x) +$
46 17.312) and $S2_{(1-1000)}$ ($y = 4.2315\ln(x) + 34.255$), respectively. Based on the available slopes we
47
48
49
50
51
52
53
54
55
56
57
58
59
60

1
2
3 also quantitated the concentration of Ni^{2+} in standard solutions and we observed a good
4 agreement of the calculated concentration values for respective standard solutions (Table 2).
5
6
7

8 **Table 2**

9
10 It is well known that the acidity of the medium play a major role in complex formation.^{32, 33}
11 Thus, the influence of pH on the complex formation and color intensity of Ni-MPMN complex
12 was investigated. In Britton–Robinson buffer of pH 3-9, a series of Ni^{2+} ($100 \mu\text{g mL}^{-1}$) solution
13 was prepared and further analyzed by the proposed method. Based on ImageJ analysis it was
14 found that the $\text{PGV}_{\text{Complex}}$ increased proportionally with raising the test solution pH (3-5) and
15 declined at higher pH (5-9) as shown in Figure 4. The solution pH also influenced $\text{PGV}_{\text{Blank}}$
16 which increased on raising the solution pH from 4-9. This background color negatively
17 influenced the assay results as the signal-to-noise (S/N) depends from the difference of
18 $\text{PGV}_{\text{Complex}}$ and $\text{PGV}_{\text{Blank}}$ values. Based on the data shown in Figure 4 (Inset), it is clear that, the
19 optimum pH of the complex (Ni-MPMN) formation lies at pH 5. Mercapto group (-SH) of the
20 reagent at pH 3-5 is dissociated easily and the reagent coordinates to Ni^{2+} ion as a monobasic
21 bidentate fashion (NS donor) through the mercapto (-SH) after deprotonation and the azomethine
22 (-C=N-) groups. (Please see SI-1, SI-2 for UV and FTIR spectra). This behavior most likely
23 accounts for the observed color change. At higher pH (>5), the instability, hydrolysis and/or the
24 incomplete complex formation of Ni-MPMN may account for the trend observed. However, in
25 our developed method we did not make any pH adjustment as Ni^{2+} solution was prepared in
26 Milli-Q water (pH 5.4).
27
28
29
30
31
32
33
34
35
36
37
38
39
40
41

42 **Figure 4**

43
44 *3.4. Selectivity and interference study*

45
46 The selectivity of MPMN reagent towards individual heavy metal ions (Ag^+ , Al^{3+} , As^{3+} ,
47 Ba^{2+} , Cd^{2+} , Cr^{3+} , Fe^{3+} , Pb^{2+} , Ni^{2+} and Mn^{2+}) was judged by our developed method. The results
48 revealed that the MPMN reagent forms strong complex formation with Ni^{2+} ions as compared to
49 aforementioned ions (Figure 5). A weak complex formation was also observed for Cd^{2+} , Cr^{3+} ,
50 Fe^{3+} and Ag^+ in the following order $\text{Cd}^{2+} > \text{Cr}^{3+} > \text{Fe}^{3+} > \text{Ag}^+$. Moreover, the stability of these
51 complexes and their color intensity was found to be low as compared to Ni^{2+} . On the other hand,
52
53
54
55
56
57
58
59
60

the concentration of the heavy metal ion was very high (i.e., $100 \mu\text{g mL}^{-1}$), and based on the color intensity it is unlikely to form a strong colored complex at concentrations below $1 \mu\text{g mL}^{-1}$.

Figure 5

The influence of potential interfering ions on the selectivity of MPMN reagent towards Ni^{2+} and assay performance was also investigated. Representative analyte ($1 \mu\text{g mL}^{-1} \text{Ni}^{2+}$) solution was tested in the presence of 10-1000 $\mu\text{g mL}^{-1}$ fold excess of a range of heavy metal (Ag^+ , Al^{3+} , As^{3+} , Ba^{2+} , Cd^{2+} , Cr^{3+} , Fe^{3+} , Pb^{2+} and Mn^{2+}) ions individually. It was found that the proposed method for detection of Ni^{2+} ions was free from the interferences of Ag^+ , Al^{3+} , As^{3+} , Ba^{2+} , Pb^{2+} and Mn^{2+} at least up to interference to analyte ratio of 1000:1 $\mu\text{g mL}^{-1}$ concentration. The tolerance limit was defined as the concentration of added species causing a relative error less than $\pm 5\%$ in the magnitude of the color intensity. An acceptable recovery ($98 \pm 2\%$) of Ni^{2+} ions was achieved without interference. Even though a weak complex formation for Cd^{2+} , Cr^{3+} and Fe^{3+} towards MPMN reagent was observed in the following order: $\text{Cd}^{2+} > \text{Cr}^{3+} > \text{Fe}^{3+}$ and their stability and color intensity were found much lower as compared to Ni^{2+} complex with the same reagent (Please see Figure 5). Thus, it can be concluded that, the reagent MPMN is highly selective towards complex formation with Ni^{2+} ions compared to most of the aforementioned ions. The possible interference from Cd^{2+} was masked by adding one drop of KI (0.01%) to the test solution, whereas the interference of Cr^{3+} was masked by adding few drops of H_2O_2 (30% (v/v)) in alkaline KOH (1.0 mol L^{-1}). The interference from Fe^{3+} was also masked by adding one crystal of NaF to form colorless and high stable $[\text{FeF}_6]^{3-}$ anionic complex compared to Ni-MPMN complex species.

The influence of commonly occurring potential harmless interfering cations e.g. Ca^{2+} , Na^+ , K^+ and anion such as Cl^- on the performance of one-step assay was also studied. A 10-fold diluted Ni^{2+} solution (10^{-2} to $10^2 \mu\text{g mL}^{-1}$) was tested in the presence of a relatively high excess ($10^3 \mu\text{g mL}^{-1}$) of the interfering ions. The results revealed that, for higher concentrations of Ni^{2+} , a drop in the PGV value was noticed (Figure 6). However, our assay results showed a negligible difference at lower analyte concentrations ($< 10^1 \mu\text{g mL}^{-1}$). Thus, it can be concluded that, these results are in line with the data reported by Hossain and Brennan³⁴ where they found no difference in the performance of paper-based assay for the detection of Hg^{2+} at lower concentrations. According to the same author's³⁴, the presence of potential interfering metallic

agents e.g. KCl ($100 \mu\text{g mL}^{-1}$) and NaCl ($200 \mu\text{g mL}^{-1}$) did not negatively influence the detection of aforesaid ion. Hence, our proposed method showed a low deviation in the presence of nontoxic interfering agents especially at a lower concentration of the tested metal ion.

Figure 6

3.5. Figures of merit

Under the optimized conditions, the calculated values of LOD³⁵ using the formula $\text{LOD} = 3S_{y/x}/b$ where $S_{y/x}$ is the standard deviation of y -residual and b is the slope of the calibration plot was found equal $0.01 \mu\text{g mL}^{-1}$. The analytical feature (LOD), of the developed method competed favorably with many of the reported methods e.g. multiplex paper sensors;^{36, 37} solid phase extraction³⁸ and solid phase extraction coupled with high performance liquid chromatography (HPLC)³⁹; dual-cloud point extraction;⁴⁰ and spectrometric methods^{33,41,42} (Table 3). The proposed method provides better LOD and ease of use and less interference (Figures 5 & 6). Some of these methods have shown high LOD and serious interferences by halide ions. Moreover, the LOD compared favorably with the LOD of GFAAS ($0.4 \mu\text{g mL}^{-1}$) and FAAS ($1.24 \mu\text{g mL}^{-1}$). Also, most of the reported methods suffered from the need of expertise for operations, time-consuming as well as expensive solvents/reagents but our proposed method offers low-cost device and easy to fabricate with no prior complex sample preparation steps; thus making it as an effective approach for measuring Ni^{2+} in environmental samples. The LOD of the method is lower than the maximum allowable level of nickel in soil (<0.7 to $47 \mu\text{g/kg}$) and solid sewage (18 to $260 \mu\text{g/kg}$) reported by World Health Organization (WHO) in water.^{43,44}

On the other hand, our developed method shows very good limit of detection, good precision and selectivity and are better and/or comparable with the reported methods (Table 3). Good preconcentration, simple sample preparation, high selectivity, low LOD as well as low-cost system would make the method suitable for measuring Ni^{2+} in various environmental samples. The method could also be extended for analysis of Ni^{2+} ions even at level $< \text{ng mL}^{-1}$ or ng g^{-1} after preconcentration of Ni from large sample volume onto solid sorbent packed column prior determination.⁴⁵

Moreover, the influence of dissolved carbon on the selectivity of the developed method by humic acid and other inorganic salts in water was also carried out as described in subsection 2.4.4. The results revealed no significant differences (I_2-I_1) in the signal intensities between the

two samples (before and after digestion). Thus, these results added further support to the good performance of the chelating agent MPMN towards complex formation with Ni^{2+} . Moreover, the results revealed that, the ligation capacity and stability constants of humic acid (as a carbon source in water and others like dissolved CO_2 , H_2CO_3 , bicarbonate salts, soluble carbonates of Na, K and NH_4^+ , and other some insoluble metal carbonates) as complexing agent towards Ni^{2+} are much lower than the ligation capacity and stability constant of the reagent MPMN towards Ni^{2+} . The fact that, the reagent MPMN has very strong binding sites (NOS) which are strong enough to replace humic acid in its Ni complexes.

The robustness test of the developed method was also performed by recording the signal intensities (i.e., PG values) after slight change in temperature and volume on the recommended procedures. The results revealed no significant differences (I_2-I_1) in the signal intensities of the sample measured by the recommended procedures (I_1) and the method after slight change in temperature and volume (I_2). This further adds support to the good performance as well as robustness of the developed method under various conditions (Please see SI-3, 4).

Table 3

3.6. Analytical application:

Because of the unavailability of certified reference materials for Ni^{2+} to explore the reliability and validity of the proposed method, the recovery tests were implemented successfully for detection and semi quantitative analysis of known concentrations of Ni^{2+} ions spiked into tap water and various wastewater samples. The water samples were spiked with known amounts of Ni^{2+} before sample preparation and subsequently analyzed by the proposed method. The results are demonstrated in Table 4. Based on color intensity and PGV analysis, the concentration of Ni^{2+} spiked to tap water sample was found equal $0.84 \mu\text{g mL}^{-1}$ (Table 4). The variation (-16%) is most likely due to the presence of nontoxic interfering species present in tap water. The fact that, high concentration of non-interfering cations and anions in the test sample solution may influence the rate and color intensity of produced colored nickel complex species as explained in section 3.4. Thus, the developed method is not only simple but also offers high selectivity with good limit of detection.

Table 4

4. Conclusions:

The application of Styrofoam modified hydrophobic paper as a platform for sensitive detection of Ni²⁺ was demonstrated. Due to low-wettability of the modified substrate, the assay sensitivity was increased by 3-order of magnitude. The present method offers a rapid yet simple detection tool which is coupled with good reproducibility, accuracy and robustness so that it can be readily used for field applications. The method can be utilized for routine analysis of Ni²⁺ in environmental water samples since most of the reported methods suffer from many drawbacks e.g. time consuming, cost, multiple steps, robustness and costly solvents (HPLC). The LOD is also lower than the maximum allowable level (MAL) of Ni²⁺ by WHO in water and favorably compared with LOD of many spectrochemical (e.g. GFAAS, FAAS and ICP-MS) and electrochemical techniques. The method could also be extended for detection and semiquantitative of ultra trace (picomolar) levels of nickel in environmental water samples via on-line preconcentration from large sample volumes onto nanosized solid phase extractor packed column prior determination.

Acknowledgements:

The authors are thankful for the support from the Center of Excellence in Environmental Studies (CEES), King Abdulaziz University and Ministry of Higher Education, Kingdom of Saudi Arabia.

References:

1. D. Beyersmann and A. Hartwig, *Archives of toxicology*, 2008, **82**, 493-512.
2. J. M. Matés, J. A. Segura, F. J. Alonso and J. Márquez, *Free Radical Biology and Medicine*, 2010, **49**, 1328-1341.
3. K. Jomova and M. Valko, *Toxicology*, 2011, **283**, 65-87.
4. J. E. O'Sullivan, R. J. Watson and E. C. V. Butler, *Talanta*, 2013, **115**, 999-1010.
5. R. Verma and B. D. Gupta, *Food Chemistry*, 2015, **166**, 568-575.
6. R. Wang, W. Wang, H. Ren and J. Chae, *Biosensors and Bioelectronics*, 2014, **57**, 179-185.
7. J. Shepard, V. R. Bhethanabotla and R. Toomey, 2005.
8. J. Gasparik, D. Vladarova, M. Capcarova, P. Smehyl, J. Slamecka, P. Garaj, R. Stawarz and P. Massanyi, *Journal of Environmental Science and Health Part A*, 2010, **45**, 818-823.
9. R. E. Luckham and J. D. Brennan, *Analyst*, 2010, **135**, 2028-2035.
10. J. F. Li, Z. L. Xu and H. Yang, *Polymers for advanced technologies*, 2008, **19**, 251-257.
11. A. W. Martinez, S. T. Phillips, M. J. Butte and G. M. Whitesides, *Angewandte Chemie (International ed. in English)*, 2007, **46**, 1318-1320.
12. L. Feng, H. Li, L.-Y. Niu, Y.-S. Guan, C.-F. Duan, Y.-F. Guan, C.-H. Tung and Q.-Z. Yang, *Talanta*, 2013, **108**, 103-108.

- 1
 - 2
 - 3
 - 4
 - 5
 - 6
 - 7
 - 8
 - 9
 - 10
 - 11
 - 12
 - 13
 - 14
 - 15
 - 16
 - 17
 - 18
 - 19
 - 20
 - 21
 - 22
 - 23
 - 24
 - 25
 - 26
 - 27
 - 28
 - 29
 - 30
 - 31
 - 32
 - 33
 - 34
 - 35
 - 36
 - 37
 - 38
 - 39
 - 40
 - 41
 - 42
 - 43
 - 44
 - 45
 - 46
 - 47
 - 48
 - 49
 - 50
 - 51
 - 52
 - 53
 - 54
 - 55
 - 56
 - 57
 - 58
 - 59
 - 60
13. L. Feng, X. Li, H. Li, W. Yang, L. Chen and Y. Guan, *Analytica Chimica Acta*, 2013, **780**, 74-80.
14. Z. Nie, C. A. Nijhuis, J. Gong, X. Chen, A. Kumachev, A. W. Martinez, M. Narovlyansky and G. M. Whitesides, *Lab on a Chip*, 2010, **10**, 477-483.
15. S. He, D. Li, C. Zhu, S. Song, L. Wang, Y. Long and C. Fan, *Chemical communications*, 2008, 4885-4887.
16. Y.-W. Lin, C.-C. Huang and H.-T. Chang, *Analyst*, 2011, **136**, 863-871.
17. M. R. Knecht and M. Sethi, *Analytical and bioanalytical chemistry*, 2009, **394**, 33-46.
18. C. H. Chao, C. S. Wu, C. C. Huang, J. C. Liang, H. T. Wang, P. T. Tang, L. Y. Lin and F. H. Ko, *Microelectronic Engineering*, 2012, **97**, 294-296.
19. M. da Silva, N. Demarquette and I. Tan, *Cellulose*, 2003, **10**, 171-178.
20. T. Songjaroen, W. Dungchai, O. Chailapakul and W. Laiwattanapaisal, *Talanta*, 2011, **85**, 2587-2593.
21. K. Abe, K. Kotera, K. Suzuki and D. Citterio, *Analytical and Bioanalytical Chemistry*, 2010, **398**, 885-893.
22. K. F. Lei, S.-I. Yang, S.-W. Tsai and H.-T. Hsu, *Talanta*, 2015, **134**, 264-270.
23. G. Rodionova, M. Lenes, Ø. Eriksen and Ø. Gregersen, *Cellulose*, 2011, **18**, 127-134.
24. K. Khanari, K. Syverud, G. Chinga-Carrasco, K. Paso and P. Stenius, *Cellulose*, 2011, **18**, 257-270.
25. L. H. Mujawar, W. Norde and A. Van Amerongen, *Analyst*, 2013, **138**, 518-524.
26. A. B. P. Lever, *Inorganic electronic spectroscopy*, Elsevier, 1984.
27. K. Nakamoto, *Infrared and Raman Spectra of Inorganic and Coordination Compounds*, Wiley Interscience, New York, 1971.
28. R. K. Parashar, R. C. Sharma, A. Kumar and G. Mohan, *Inorganica Chimica Acta*, 1988, **151**, 201-208.
29. R. Ekins and F. W. Chu, *Trends in Biotechnology*, 1999, **17**, 217-218.
30. M. F. Templin, D. Stoll, M. Schrenk, P. C. Traub, C. F. Vöhringer and T. O. Joos, *Trends in Biotechnology*, 2002, **20**, 160-166.
31. L. H. Mujawar, A. Van Amerongen and W. Norde, *Talanta*, 2012, **98**, 1-6.
32. H. R. Rajabi, M. Shamsipur, M. M. Zahedi and M. Roushani, *Chemical Engineering Journal*, 2015, **259**, 330-337.
33. H. R. Rajabi and S. Razmpour, *Spectrochimica Acta Part A: Molecular and Biomolecular Spectroscopy*, 2016, **153**, 45-52.
34. S. M. Z. Hossain and J. D. Brennan, *Analytical Chemistry*, 2011, **83**, 8772-8778.
35. J. C. Miller and N. Miller, *Statistics for Analytical Chemistry*, Pearson Education Limited Prentice Hall, 6th edn., 2010.
36. D. M. Cate, W. Dungchai, J. C. Cunningham, J. Volckens and C. S. Henry, *Lab on a Chip*, 2013, **13**, 2397-2404.
37. D. M. Cate, S. D. Noblitt, J. Volckens and C. S. Henry, *Lab on a Chip*, 2015, **15**, 2808-2818.
38. P. Azizi, M. Golshekan, S. Shariati and J. Rahchamani, *Environmental monitoring and assessment*, 2015, **187**, 1-11.
39. Q. Zhou, A. Xing and K. Zhao, *Journal of Chromatography A*, 2014, **1360**, 76-81.
40. L. Zhao, S. Zhong, K. Fang, Z. Qian and J. Chen, *Journal of hazardous materials*, 2012, **239**, 206-212.
41. H. Zheng, B. Jia, Z. Zhu, Z. Tang and S. Hu, *Analytical Methods*, 2014, **6**, 8569-8576.
42. M. Ghaedi, B. Karami, S. Shamsaldini and M. Soylak, *Journal of Saudi Chemical Society*, 2014, **18**, 674-680.
43. W. H. O. (WHO), *Environmental Health Criteria*, Geneva, 2002.
44. G. F. Nordberg, B. A. Fowler and M. Nordberg, *Handbook on the Toxicology of Metals*, Academic Press, 2014.
45. A. B. Farag, M. H. Soliman, O. S. Abdel-Rasoul and M. S. El-Shahawi, *Analytica Chimica Acta*, 2007, **601**, 218-229.

FIGURE CAPTIONS:

Figure 1: Chemical structure of MPMN reagent (A) and Ni-MPMN complex (B)

Figure 2: AFM data for pristine and polystyrene modified Whatman filter paper showing (A) Height data (B) 3D image (C) average roughness (R_a) (D) Root mean square roughness (R_q) (E) Stiffness ($N\ m^{-1}$) and (F) Adhesion ($\times 10^{-18}J$).

Figure 3: Average pixel gray volume (PGV) comparison and performance for the Ni^{2+} ions determination of one step assay spots on non-modified pristine filter paper (A), polystyrene based hydrophobic paper (B).

Figure 4: Effect of pH on the PGV of complex (Ni-MPMN) and blank spots. Inset shows signal-to-noise ratio ($PGV_{Complex} - PGV_{Blank}$) of the assay at various pH.

Figure 5: Specificity of MPMN reagent towards Ni^{2+} ions as compared to other selected heavy metals ions.

Figure 6: Average pixel gray volume (PGV) comparison for the Ni^{2+} ions (10^2 - 10^{-2} $\mu g/mL$) determination assay spots on polystyrene based hydrophobic paper showing interference with cations (Na^+ , K^+ , Ca^{2+}) and anions (Cl^-).

LIST OF TABLES:

Table 1: Details of reagent and its Ni²⁺ complex spots on pristine and hydrophobic paper[†]

Parameter	Reagent	Ni ²⁺	Coverage (%)
	Surface area (mm ²)		
	1000 µg mL ⁻¹		
Pristine	14.3±1.1	14.3±1.1	100
Hydrophobic	16.9±2.3	7.2±0.6	57.0±3.0
	100 µg mL ⁻¹		
Pristine	15.2±0.1	15.3±0.2	100
Hydrophobic	17.4±1.4	6.7±0.1	60.5±3.4

[†] Average ± standard deviation, (n=3).³⁵

Table 2: Analysis of Ni²⁺ ions in deionized water using slopes S1[†] and S2

Concentration (µg mL ⁻¹)		P-value ^{††}	Error (%)	Slope
Standard	Calculated			
0.01	0.01±0	0.051	0	S1
0.10	0.07±0.01	0.073	-33	S1
1.00	1.22±0.49	0.099	+22	S1
10.00	9.67±2.09	0.017	-3	S2
100.00	106.88±25.41	0.088	+7	S2
1000.00	967.49±22.67	0.034	-3	S2

[†]S1: $y = 3.1633 \ln(x) + 17.312$ and S2: $y = 4.2315 \ln(x) + 34.255$.

^{††} P-value obtained from t-test at 95% confidence level. Error (%) is estimated from the mean values (n=3) of standard and calculated concentration.³⁵

Table 3: A comparison between the limit of detection of the developed and some of the reported methods for Ni²⁺ determination in water

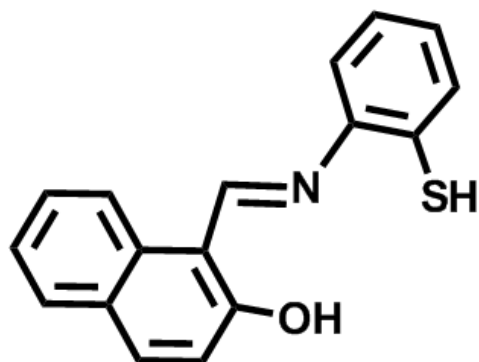
Method	LOD ($\mu\text{g mL}^{-1}$)	Remarks	Reference
Multiplex paper sensor	0.7/1.0	Time consuming and fabrication of microfluidic channels is needed	36,36
Solid phase extraction	0.03	Expensive and requires ferromagnetic nanoparticles	38
Fluorometric	1.0	Required fluorescence reader	12
Dual-cloud point extraction	0.01	Time consuming with expensive instrumentation	40
Solid phase extraction coupled with HPLC	0.04	Time consuming, required complex methodology and not applicable for routine work	39
Wavelength-dispersive X-ray fluorescence spectrometry	0.001	Sensitive but complex and requires expensive instrumentation	41
Flame atomic absorption spectrometry	0.003	Not suitable for field and routine applications	42
Spectrophotometric	0.001	Sensitive, nanobeads is needed	33
Proposed Styrofoam modified paper method	0.01	Low-cost, precise, rapid, selective and applicable for routine analysis	Present work

Table 4: Analytical utility of the developed Styrofoam modified paper for determination of nickel in various water samples (n=3)

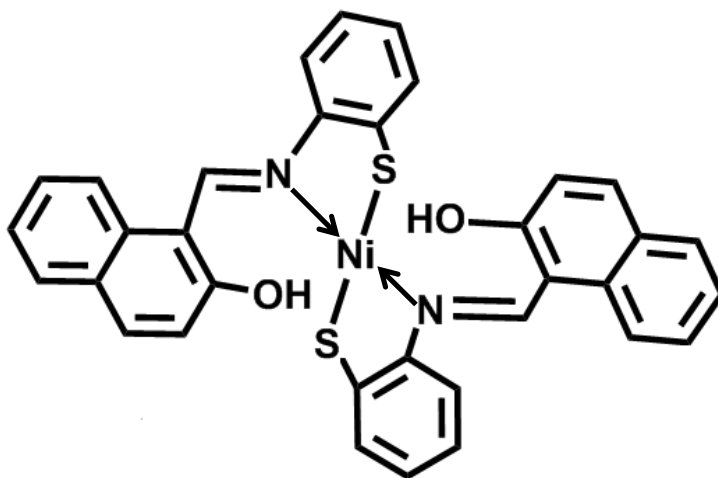
Sample	PGV	Ni ²⁺ (µg mL ⁻¹)
Tap water	7.15 ± 1.16	0.04 ± 0.01
Tap water (spiked with Ni ²⁺)	16.76 ± 0.23	0.84 ± 0.06
Wastewater 1	6.32 ± 0.83	0.03 ± 0.01
Wastewater 2	3.73 ± 0.82	0.01 ± 0.00
Wastewater 3	6.05 ± 1.38	0.03 ± 0.02
Wastewater 4	5.64 ± 0.17	0.03 ± 0.00

† Average of three measurements ± standard deviation.³⁵

Figure 1



A



B

Figure 2

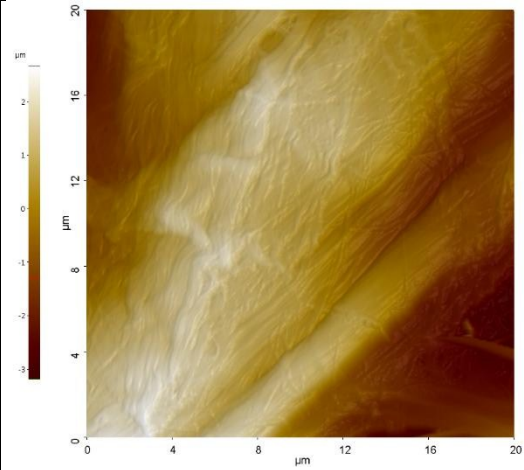
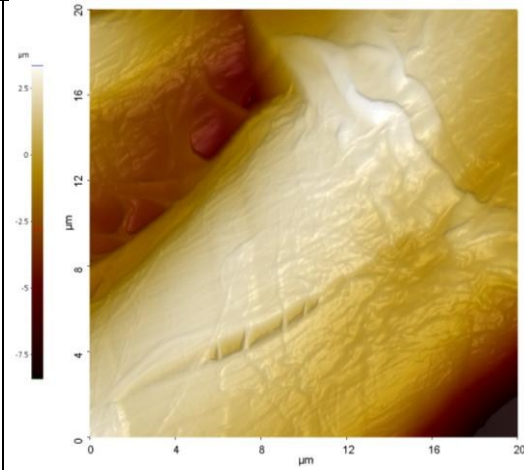
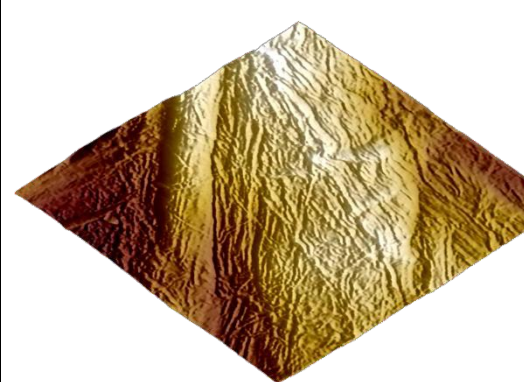
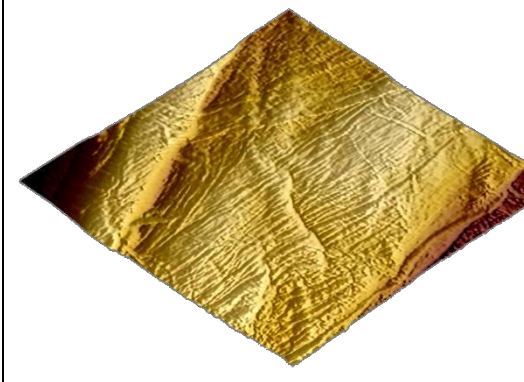
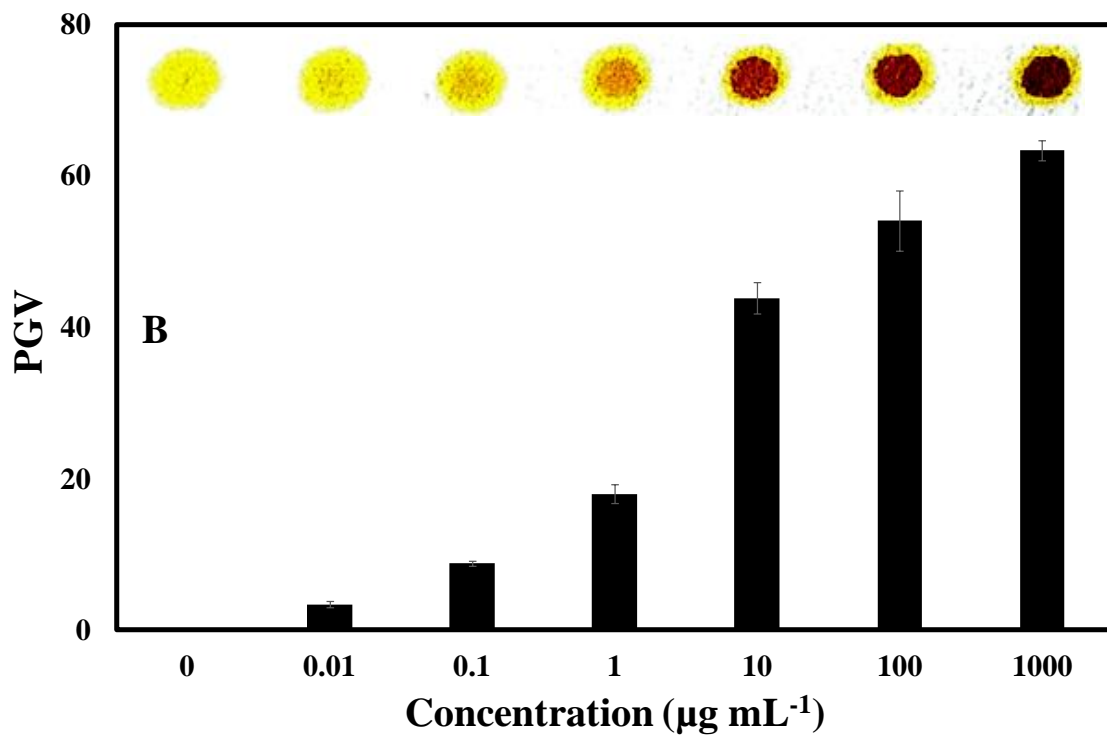
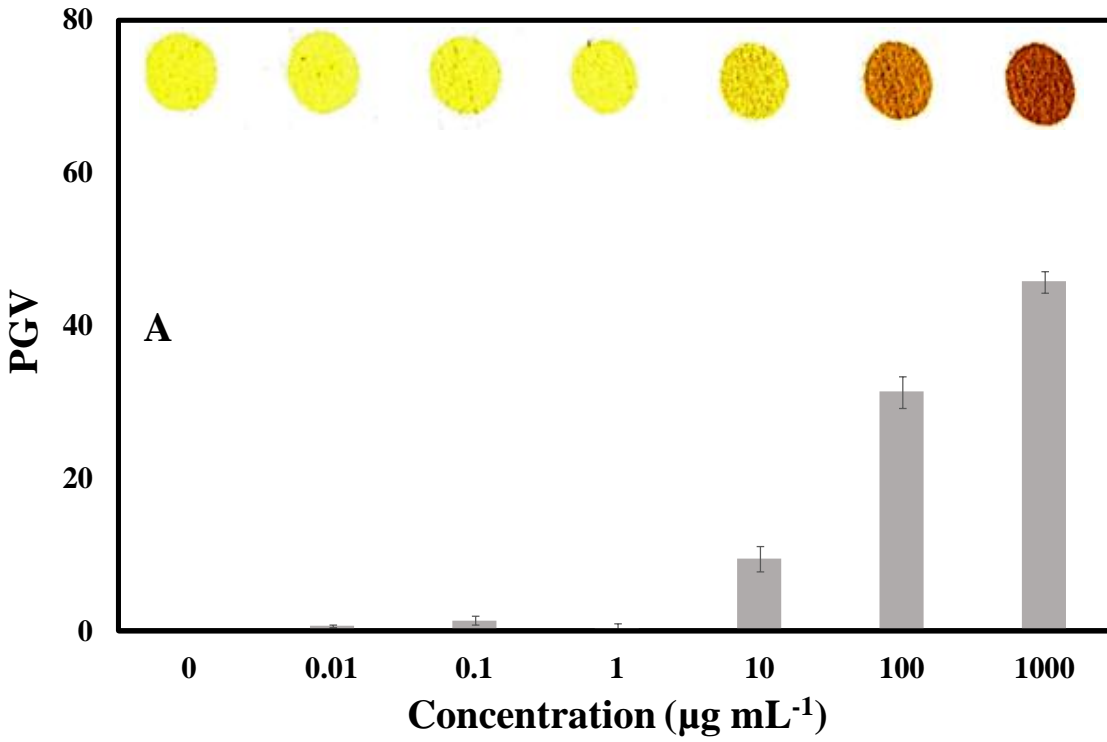
Parameters	FILTER PAPER	
	Pristine	Styrofoam modified
(A) Height (2D) (20×20μm)		
(B) 3D image (20×20μm)		
(C) R_a	94	178
(D) R_q	128	225
(E) Stiffness ($N m^{-1}$)	1.583	1.718
(F) Adhesion ($\times 10^{-18} J$)	53.54	84.69

Figure 3



Analytical Methods Accepted Manuscript

Figure 4

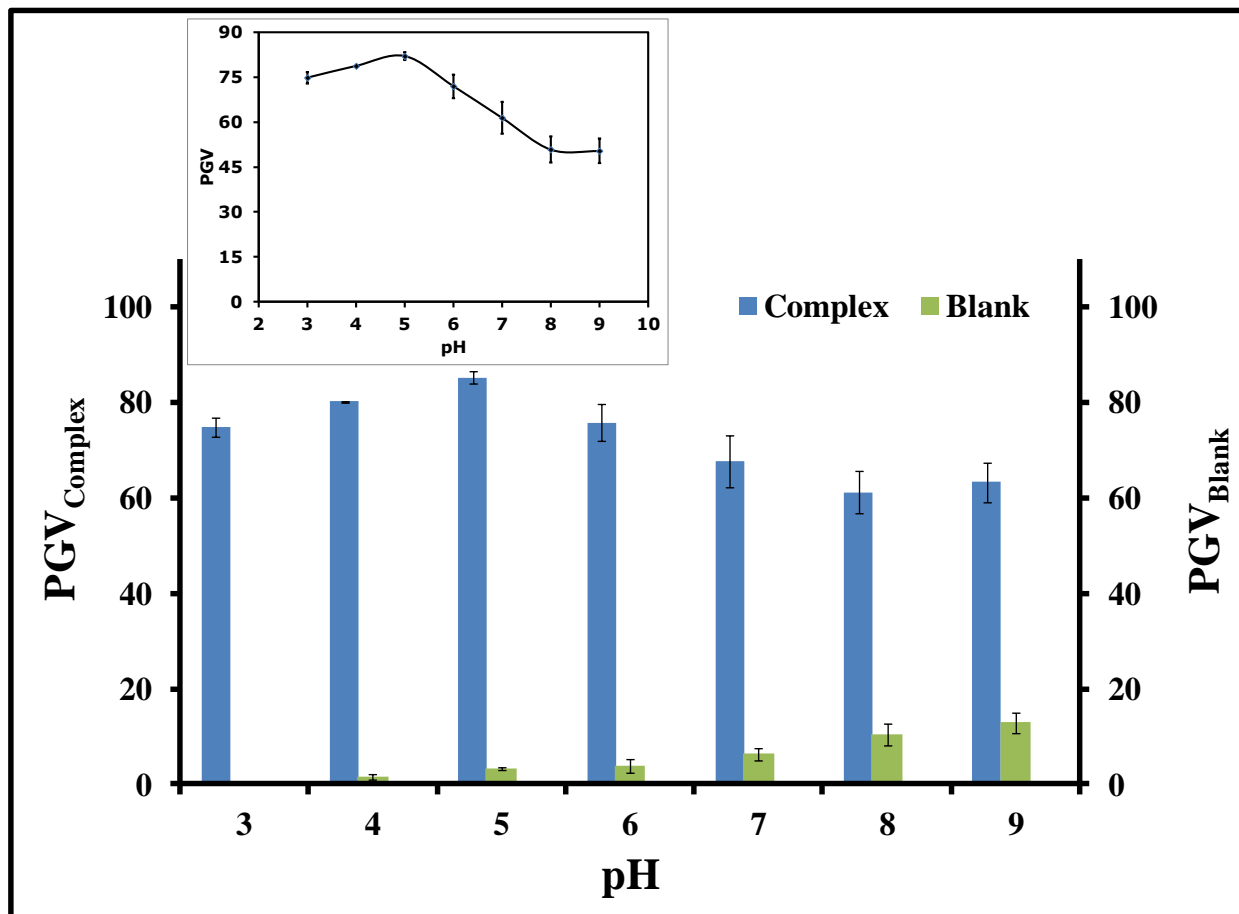


Figure 5

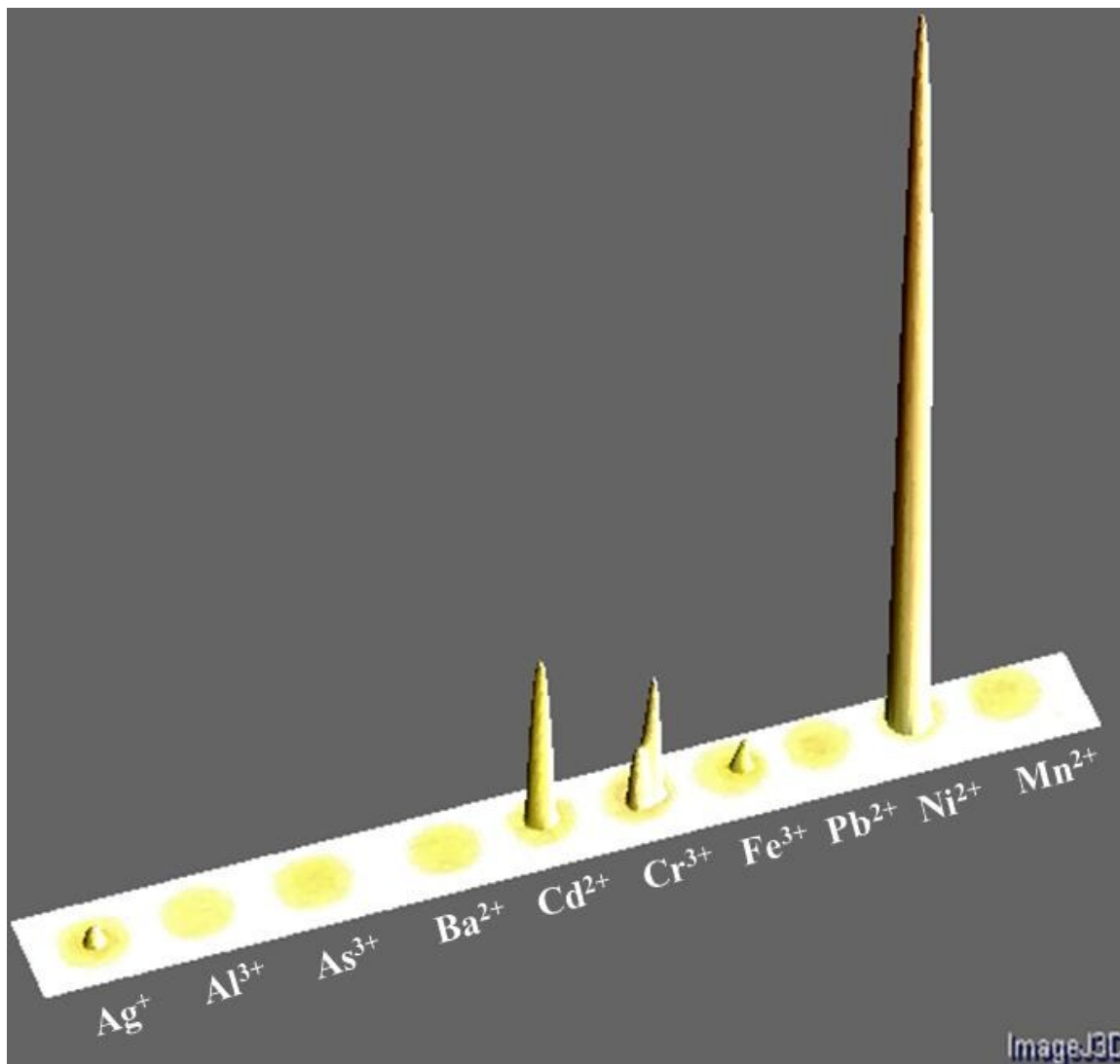
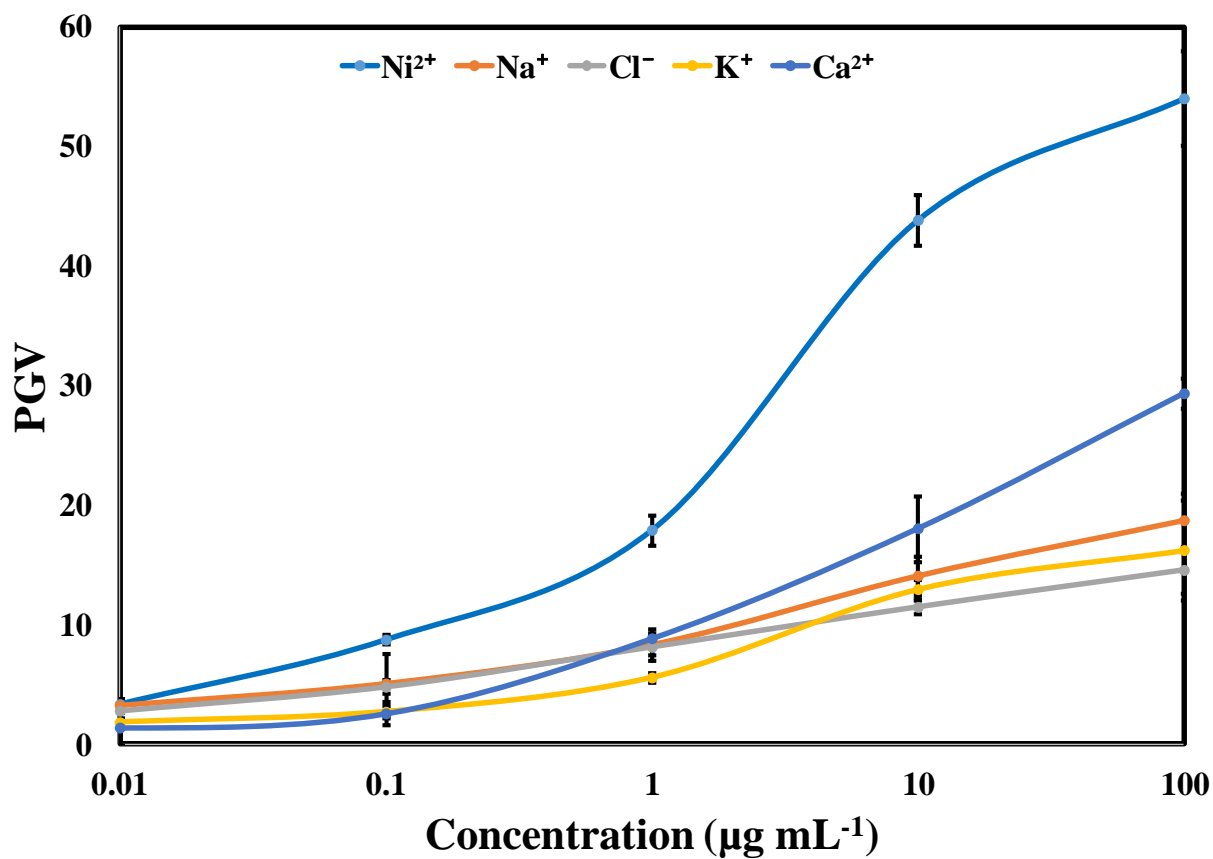
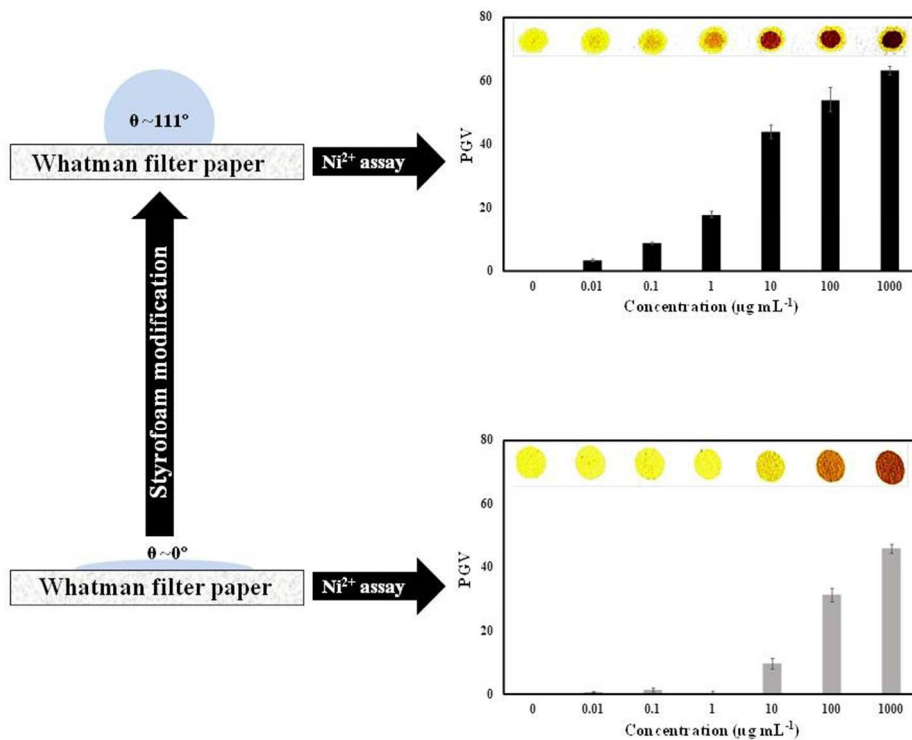


Figure 6





254x190mm (96 x 96 DPI)

1
2
3
4
5
6
7
8
9
10
11
12
13
14
15
16
17
18
19
20
21
22
23
24
25
26
27
28
29
30
31
32
33
34
35
36
37
38
39
40
41
42
43
44
45
46
47
48
49
50
51
52
53
54
55
56
57
58
59
60